ARTICLES

Friction and noise-induced coherent structures in boundary lubrication

I. Tovstopyat-Nelip and H. G. E. Hentschel
Department of Physics, Emory University, Atlanta, Georgia 30322
(Received 21 September 1999)

We examine the effect of stick-slip boundary conditions on the friction generated by a molecularly thin layer of a liquid lubricant separating two plates. For one-dimensional compressible flows, noise-induced coherent dissipative structures on a micron scale are generated due to cooperation between the external drive and the thermal noise. As a function of the thermal noise these structures show a peak in their amplitudes similar to stochastic resonance. At low velocities a reduction in friction with increasing thermal noise is observed.

PACS number(s): 47.52.+j, 83.50.Gd, 83.50.Ws, 68.15.+e

I. INTRODUCTION

The study of friction between two surfaces is a very old problem, but an extremely important one from a technological point of view [1–4]. This is especially true on the mesoscopic scale, where, despite significant efforts made in recent years, much remains to be understood about the fundamental processes responsible for friction and lubrication. New experimental methods such as the quartz crystal microbalance [5] and the surface-force apparatus [6–11] have, however, provided new insights into the nanoscale and mesoscale processes occurring during dissipation at interfaces, and stimulated a great deal of theoretical research [12–16].

It is common to distinguish hydrodynamic lubrication from boundary lubrication. In the first case, the layer of fluid between the sliding plates is relatively thick, and the friction can be calculated straightforwardly from the Navier-Stokes equations with stick boundary conditions. The case of boundary lubrication, however, when the lubricating layer is molecularly thin, has a much more complex dynamics. Common theoretical approaches to this problem include studies of nonlinear dynamical systems consisting of several particles moving between two plates [12–14], and molecular dynamics simulations of ensembles of a finite number of particles [15,16].

While fluids retain their bulk shear flow properties when the thickness of the lubricating film is more than about ten molecular diameters, recent studies show that confined thin film fluids display strong viscoelastic characteristics, slow relaxation, and solidlike behavior to the point where the elastic forces significantly exceed the viscous ones [8,9,11,7,4]. At the same time, it is known experimentally that even one molecular layer of a fluid can significantly reduce the interfacial friction [17]. A liquid in such an extreme state of confinement can exist in a variety of differently ordered states depending on the temperature and the sliding velocity [3], and dynamic phase transitions such as shear melting can occur during sliding. The reason for, and the nature of, such slowed down dynamics in confined fluids is still not fully understood, and its nonequilibrium structure remains to be elucidated [11,4].

At the mesoscopic scale stick-slip boundary conditions, represented by velocity-weakening effective interactions [18,19] between the confined fluid film and the interface, can be expected to significantly affect their hydrodynamic behavior. In this paper we therefore study the compressible hydrodynamic behavior of a molecularly thin fluid layer between two sliding plates in which the dominant interactions are these velocity-weakening forces. Because of the complexity of the problem, we only consider a one-dimensional version of the fluid evolution. Numerical simulations of the resulting equations of motion show that the complex dynamics of the system gives rise to the appearance of a coherent dissipative microscale structure in a fluid which was tentatively predicted by Demirel and Granick [10,4]. Also, we observed a reduction in friction at low velocities with increasing temperature.

The scheme of the paper is as follows. In Sec. II we describe our model. Section III is devoted to a presentation and discussion of our numerical simulations. In Sec. IV we discuss the relationship between the temperature of the confined fluid layer and the strength of the random thermal force acting on it. Section V concludes the paper with a summary and discussion of our results.

II. STICK-SLIP HYDRODYNAMICS

The presence of stick-slip boundary conditions at the mesoscale is a direct result of the strong intermolecular forces that exist between a sliding thin film and the surface layer at the atomic scale. There exists strong evidence that the stick forces on ordered arrays are much larger when the array is interacting with a commensurate substrate than with an incommensurate one [1,20,21]. The underlying reason for this is clear: when the lattice is commensurate each atom can lie in a potential minimum of the substrate. For an incommensurate lattice strong frustration occurs as the atoms in the ordered array try to accommodate both their interatomic interactions and their atom-substrate interactions, leading to commensurate-incommensurate transitions [22]. Studies of the influence of such interactions using the dynamic Frenkel-Kontorova model lead to the conclusion that velocity weakening stick-slip forces are a generic consequence of such interatomic interactions [12,13]. Indeed, such stick-slip boundary conditions are not limited to the nanoscale, and in

macroscopic investigations of dry friction [23–25] at low velocities the dynamics was also usually characterized by intermittent periods of stick and slip. Several dynamical transitions have been found in such macroscopic investigations including a supercritical Hopf bifurcation between stick-slip and steady sliding, and hysteresis due to subcritical Hopf bifurcations.

Investigations of the consequences of such velocity-weakening interactions have already been used in the context of earthquake models [18,19,26] involving the dynamics of sets of elastically coupled driven blocks interacting with a substrate via singular velocity weakening friction forces. The dynamics of the earthquake models is described by coupled sets of ordinary nonlinear differential equations. Driven thin films also show strong viscoelastic characteristics, which means that their dynamics should be described by the hydrodynamics of compressible fluid, while the strong stick-slip interactions will lead to strong velocity weakening stresses at the interface.

In principle, the general form of the elastohydrodynamic equations that needs to be investigated to understand the behavior of the driven thin film is, therefore,

$$\rho \partial v_\alpha / \partial t + \rho \vec{v} \cdot \vec{\nabla} v_\alpha = -\partial p / \partial x_\alpha - \partial \tau_{\alpha\beta} / \partial x_\beta + \rho G_\alpha(\vec{x},t),$$
$$\partial \rho / \partial t + \vec{\nabla}(\rho \vec{v}) = 0, \tag{1}$$

where $\tau_{\alpha\beta}$ is the stress tensor in the thin film, while the last term $[G_\alpha(\vec{x},t)]$ on the right hand side of Eq. (1) represents the thermal noise which has Gaussian statistics $\langle G_\alpha(\vec{x}_1,t_1) G_\beta(\vec{x}_2,t_2)\rangle = \Gamma \delta_{\alpha\beta} \delta(\vec{x}_1 - \vec{x}_2)\delta(t_1 - t_2)$.

The stress tensor will have strong viscoelastic characteristics, resulting in a relationship between the rate of strain $\partial v_\alpha / \partial x_\beta$ and the stress $\tau_{\alpha\beta}$ of the form

$$\partial v_\alpha / \partial x_\beta = (1+\sigma)/E \, d\tau_{\alpha\beta}/dt + (\tau_0/\eta) F(\tau/\tau_0), \tag{2}$$

where σ is Poisson's ratio, E is Young's modulus, η is the dynamic viscosity of the film, and τ_0 is a stress scale such that, for $\tau \ll \tau_0$, the film behaves as a viscous fluid. For non-Newtonian fluids typical parametrizations might include the Eyring-Ree form $F(x) = \sinh(x)$.

The basic stick boundary conditions for bulk flows need to be replaced by nonlinear velocity weakening shear stresses $\tau_{xz}(v_x)$ and $\tau_{yz}(v_y)$ at the boundaries of the driven thin film. For example, a typical velocity weakening stress would be $\tau(v) = \sigma_0 f(v/c)$, where $f(u) = 1/[bu + \mathrm{sgn}(u)] + Ku$, and c is the speed of sound in the compressible thin film. Thus, in addition to the boundary conditions $v_z(x,y,z=0,t) = 0$ and $v_z(x,y,z=H,t) = 0$, there exist the nonlinear velocity weakening boundary conditions for the components of the velocity parallel to the interface:

$$\eta \partial v_\parallel(x,y,z=0,t)/\partial z = \tau(v_\parallel(x,y,z=0,t)),$$
$$\eta \partial v_\parallel(x,y,z=H,t)/\partial z = \tau(v_\parallel(x,y,z=H,t) - V), \tag{3}$$

where V is the velocity of the upper plate.

Clearly the complexity and nonlinearity of Eqs. (1)–(3) will lead to large number of different spatiotemporal phenomena depending on driving, thermal noise, and material properties of the thin film. However, in this paper we wish to understand the most basic phenomena that such stick-slip interactions can induce in the driven hydrodynamics of thin films by looking at a one-dimensional version of the hydrodynamics in which a velocity-dependent friction force $F(v)$ between a plate and the layer of a liquid lubricant, shown schematically by the solid line on Fig. 1, replaces the full effect of the boundary conditions.

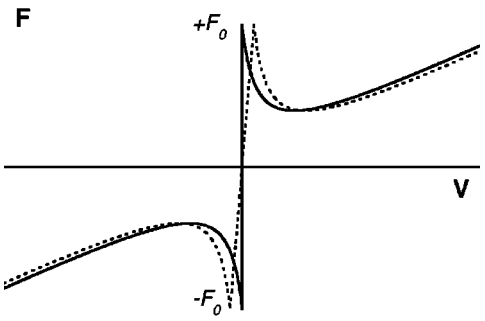

FIG. 1. The velocity weakening friction force $F(v)$ between a plate and the layer of a lubricant as a function of v.

The function $F(v)$ ranges between $\pm F_0$ at zero velocity, decreases monotonically as the velocity grows, and begins to grow linearly after some characteristic velocity v_0 (the apparent discontinuity at $v=0$ should be considered as the limit case of a continuous dependence at velocities $v \ll v_0$ shown on Fig. 1 by the dotted line). The force $F(v)$ acts like a body force in our one-dimensional model. It can be considered as a coarse-grained representation of the complex stick-slip boundary conditions. It is this force which is the basic source of nonlinearity in the model and leads to the complex spatiotemporal dynamics exhibited by the thin film.

The velocity $v(x,t)$ and the density $\rho(x,t)$ in the driven film are therefore given by

$$\rho \partial v/\partial t + \rho v \, \partial v/\partial x + c^2 \partial \rho/\partial x = -\rho[F(v) + F(v-V)] + \rho G(x,t), \tag{4}$$

$$\partial \rho/\partial t + \rho \partial v/\partial x + v \, \partial \rho/\partial x = 0. \tag{5}$$

Here $c^2 = \partial p/\partial \rho$ is the square of the speed of the sound, which may of course be very different from that observed in the bulk fluid, and which we treat as a constant corresponding to the average compressibility of the thin film in the longitudital direction. This assumption is valid provided the density fluctuations are much less than the average density, which indeed turns out to be the case. The sum of two force terms $[F(v) + F(v-V)]$ on the right hand side of Eq. (4) represents the interaction (force and unit mass) of a fluid with both plates, one plate being at rest and another one moving with a velocity V. We parametrize the functional dependence of $F(v)$ as

$$F(v) = F_0 f(v/c), \tag{6}$$

where $f(u) = 1/[bu + \mathrm{sgn}(u)] + Ku$. This form of the function $F(v)$ corresponds to the solid line in Fig. 1.

The last term on the right hand side of Eq. (4) represents the thermal noise which is taken to be uncorrelated and Gaussian:

$$\langle G(x_1,t_1)G(x_2,t_2)\rangle = \Gamma\,\delta(x_1-x_2)\,\delta(t_1-t_2). \tag{7}$$

As the fluctuation-dissipation theorem tells us that the coefficient Γ in Eq. (7) is proportional to the temperature, in this paper we use Γ as a measure of the temperature. We will elaborate on the relationship between Γ and the real temperature below in Sec. III.

Equation (4) does not contain a viscosity term. This corresponds to one of our basic simplifying assumptions that the dynamics of the thin film is dominated by nonlinear interfacial interactions, and that the elastic forces in the film are more important then the viscous ones. This appears to be reasonable for very thin films, and strong stick-slip boundary conditions. We have verified this by doing simulations in a presence of viscosity, and found that it does not make a significant contribution to the dynamics of the system for experimentally reasonable values. Naturally, for thick films this assumption must break down.

If we take the plates in our problem to be of macroscopic size, then the dimensional parameters in the model are the speed of sound $[c]=L/T$ with dimensions of velocity, the driving velocity $[V]=L/T$ with units of velocity, $[F_0]=LT^{-2}$ with dimensions of acceleration, and the noise strength $[\Gamma]=(L/T)^3$ with dimensions of velocity cubed. Using the material parameters c and F_0 to define units of length $L=c^2/F_0$ and time $T=c/F_0$, we are left with two dimensionless parameter, the scaled driving velocity $V'=V/c$ and the effective thermal noise strength $\Gamma'=\Gamma/c^3$, describing the influence of the environment on the dynamics.

Let us estimate the orders of magnitude of these scales of length L and time T. In Ref. [10] a modified surface force apparatus technique was applied to the study of friction between two atomically smooth crystals of muscovite mica separated by a molecularly thin film of squalane. The film thickness in this experiment was 18 Å, which constituted several molecular layers, the diameter of the contact interface was ≈ 45 μm, and the value of the external oscillatory driving force was $\approx 10^2$ μN. Thus the typical accelerations applied to the film during the experiment were $F_0 \approx 10^{10}-10^{11}$ m/sec^2, while a reasonable estimate of the speed of sound in such films is $c \approx 10-100$ m/sec. We therefore obtain a typical length scale in the experiment of $L=c^2/F_0 \sim 10^{-2}-1$ μm and time scale $T=c/F_0 \sim 10^{-9}-10^{-8}$ sec. These length and time scales are much larger than the atomic length (~ 10 Å) and time ($\sim 10^{-12}$ sec) scales, and suggest that nontrivial hydrodynamic phenomena might appear at such scales, in agreement with the observation of Demirel and Granick that the broad power law distributions in the frictional forces generated by molecularly thin films upto 2 nm thick might be due to long lived spatially coherent stuctures in the thin film [4]. It is the possibility of the existence of such coherent stuctures that we are interested in investigating.

To do this we first divide Eqs. (4) and (5) by ρ, and use instead of ρ the logarithmic density $m=\log(\rho/\rho_0)$, where ρ_0 is the average density in the film. In addition, we make a transition to the dimensionless variables $x'=x/L$, $t'=t/T$, and $v'=v/c$. The dimensionless equations for the velocity $v(x,t)$ and the logarithmic density $m(x,t)$ (all primes now omitted henceforth) are therefore

$$\partial v/\partial t + v\,\partial v/\partial x + \partial m/\partial x = -[f(v)+f(v-V)] + G(x,t), \tag{8}$$

$$\partial m/\partial t + \partial v/\partial x + v\,\partial m/\partial x = 0. \tag{9}$$

Since we consider the system described by Eqs. (8) and (9) as infinite in space, we do not introduce any boundary conditions, but will rather study the initial value problem starting from some initial condition $v_0(x), m_0(x)$.

The only dimensionless parameters in our model, which we still have to set are b and K in $f(u)$ [Eq. (6)]. The parameter b determines the rate of ''velocity weakening,'' and K gives the rate of the increase of the force for large velocities. Specifically, the minimal velocity occurs at $v_0/c=(\sqrt{b/K}-1)/b$. These parameters are material dependent. As we expect, $v_0/c \ll 1$; we chose them to have the physically reasonable values $b=100$ and $K=2$ which fixes $v_0/c \approx 0.06$, and use these values throughout this paper.

III. TEMPERATURE AND STRENGTH OF THE THERMAL NOISE

The explicit relationship between Γ which describes the influence of the thermal environment on the dynamics of the confined fluid layer and temperature T can be established in the case of stick-slip hydrodynamics by generalizing the formalism of hydrodynamic fluctuations introduced by Landau and Lifshitz [27]. We have to determine the rate of change of the total entropy $\dot{S}$ of the fluid, from which it is possible to find the coefficient Γ for the correlation function (7).

Taking into account the equation of heat transfer,

$$\rho T(\partial s/\partial t + v\,\partial s/\partial x) = 2\rho v F(v), \tag{10}$$

which, together with two dynamic equations (4) and (5), constitutes the complete system of hydrodynamic equations, for the production of entropy in the layer we obtain

$$\dot{S} = \int \frac{2}{T}\rho v F(v)\,dL. \tag{11}$$

In Eq. (10), s is the entropy of the fluid per unit mass, and the integration in Eq. (11) is done over all the whole fluid layer. In Eqs. (10) and (11) we are measuring temperature in energy units ($k_B=1$), and we have neglected the thermal flow term in Eq. (10), assuming that the temperature gradients in the system are small.

Having found $\dot{S}$, we can determine the correlation function of the thermal stochastic force $G(x,t)$; we obtain

$$\langle G(x_1,t_1)G(x_2,t_2)\rangle = \frac{TF(v)}{\rho v}\,\delta(x_1-x_2)\,\delta(t_1-t_2). \tag{12}$$

For the hydrodynamic description to be valid we have to assume that the velocity fluctuations are much smaller than the mean hydrodynamic values of the velocity. This means that v in Eq. (12) cannot be less than v_T, the amplitude of thermal velocity fluctuations. As, however, in the most interesting region v is of order of magnitude of the velocity of the external drive $V \gg v_T$, to a good approximation we can replace Eq. (12) by

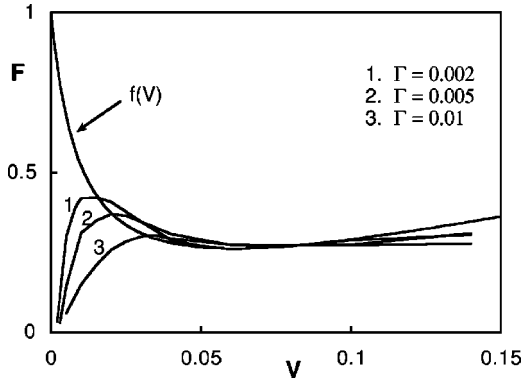

FIG. 2. The effective temperature dependent friction forces $F_{fr}(V)$ for three different temperatures. $\Gamma=0.002$, 0.005, and 0.01.

$$\langle G(x_1,t_1)G(x_2,t_2)\rangle = C\frac{TF_0}{\rho_0 V}\delta(x_1-x_2)\delta(t_1-t_2), \tag{13}$$

where C is a constant of order of magnitude of 1. Substituting into Eq. (13) a room temperature for T, $V\sim 0.1c$ and $\rho_0\sim 10^{-9}$ g/cm—typical values for one monolayer—and F_0 and c estimated in Sec. II, we obtain $\Gamma'=\Gamma/c^3\sim 10^{-3}$, the characteristic order of magnitude used in our simulations.

We emphasize once again that in the case when v and ρ fluctuate strongly enough, and amplitudes of their fluctuations exceed corresponding average values, the hydrodynamic description is not valid. For our problem this is the case of small V and relatively large temperatures. Nevertheless, our results in this range of parameters seem to be qualitatively reasonable: the linear dependence of F_{fr} on V and decreasing of F_{fr} with increasing Γ; see Fig. 2. A reasonable macroscopic description of this region of parameters can then be done within linear response theory.

IV. NUMERICAL RESULTS

Let us first consider Eqs. (8) and (9) without the stochastic term. For sufficiently low velocities of the upper plate $V<V_1^*$, where $V_1^*=2(\sqrt{b/K}-1)/b\equiv 2v_0/c$ (in our case $V_1^*\approx 0.12$), the system has three stationary solutions in the domain $0\leqslant v(x)\leqslant V$ corresponding to constant distributions of density and velocity:

$$v(x)=0, \quad m(x)=0, \tag{14a}$$

$$v(x)=V, \quad m(x)=0, \tag{14b}$$

$$v(x)=V/2, \quad m(x)=0. \tag{14c}$$

Note that if the existence of solutions (14a) and (14b) is not immediately obvious for the singular form of $F(v)$, then it becomes clear when we regard $F(v)$ as a limit of a continuous function.

Linear stability analysis shows that the first two solutions are stable, and that they are attractors of the system. They represent the film sticking to the static lower or moving upper plate, respectively. The third solution is unstable and represents the whole fluid moving with the average velocity of the upper and lower plates.

When the velocity of the upper plate reaches V_1^*, a pitchfork bifurcation in the dynamics occurs: solution (14c) becomes stable and two new fixed point solutions emerge,

$$v(x)=V/2\pm u_0, \quad m(x)=0, \tag{15}$$

which are both unstable with $u_0=\sqrt{(V/2+1/b)^2-1/(bK)}$. This situation exists for driving velocities $V_1^*<V<V_2^*$, where $V_2^*=1/K-1/b$ (note that $V_1^*<V_2^*$ for $K<b$; in our case, $V_2^*=0.49$). Finally, for $V>V_2^*$ the two stick solutions disappear and we end up with only one stationary solution [Eq. (14c)] which is stable. Thus we are dealing with a subcritical pitchfork bifurcation at $V=V_1$ if we take as our control parameter $r=(V_1-V)/V_1$.

Numerically we can show that in the case $V<V_1^*$ (or $r>0$) any initial conditions with a constant density and $v_0(x)<V/2$ for all x belongs to the basin of attraction of solution (14a), and the film will stick to the lower plate. Conversly, the set of initial conditions with $v_0(x)>V/2$ for all x belongs to the basin of attraction of Eq. (14b), and the film will ultimately stick to the upper moving plate. But initial distributions of $v(x)$, crossing the line $v(x)=V/2$, do not evolve to any stationary attractor, and as we shall see the distributions evolve into mesoscopic scale fluctuating coherent structures. The same is true for higher velocities of the upper plate $V_1^*<V<V_2^*$ (or $r^*<r<0$) though the basins of attraction of solutions (14a) and (14b) are now determined not by $V/2$, but by $V/2-u_0$ and $V/2+u_0$, respectively.

We are interested in calculating the resulting friction force acting on the moving plate $F_{fr}(V)$. It is this quantity which will control dynamics of the upper plate when pulled across the lubricated surface. The dimensionless force per unit mass is given by the integral (in order to obtain the real force per unit mass we have to multiply it by F_0)

$$F_{fr}(V)=\frac{1}{L_{plate}}\int_0^{L_{plate}} dx\, e^{m(x)} f(v(x)-V), \tag{16}$$

where L_{plate} is the size of the upper plate. Our simulations show that, in agreement with the experimental results of Demirel and Granick [10], the friction fluctuations do not average to a constant value over the large contact area of the experiment, but coherent dissipative structures at mesoscopic scale dominate the dynamics.

It can easily be seen that if the system is found in one of the attractive stick phases (14a) and (14b), the resulting friction $F_{fr}(V)$ coincides with $f(V)$, the basic force of interaction between a plate and the layer from Eq. (6). Otherwise, if the system does not evolve to any of these attractors, the resulting force $F_{fr}(V)$ will be quite different from $f(V)$. For instance, in the case $V<V_1^*$, the simplest nontrivial initial distribution $v_0(x)$, crossing the line $v(x)=V/2$ just once, evolves to a stable ''kinklike'' solution. The velocity profile of this kink moves in the liquid with a speed close to the speed of the sound c. The velocity of the moving plate in this simulation was chosen at $V=0.01$ (in units of c). The calculation of the effective friction force for this solution gives $F_{fr}(V=0.01)=0.29$, which drastically differs from $f(V=0.01)=0.52$.

Note that although we choose the velocity V of the upper plate to be a constant, we would expect the results we now

describe to be valid even when the dynamics of the upper plate is not steady. This ''adiabatic'' point of view is justified by the fact that the time scale T of our problem is typically very small with respect to a time scale τ characterizing the motion of the upper plate (for instance, for the frequency of the external drive 1 kHz, $\tau \sim 10^{-3}$ sec$\gg T$).

In the absence of thermal noise, if the confined fluid is taken to be initially at rest with $v_0(x)=0$ and $m_0(x)=0$, it will always stay in the basin of attraction of this attractor (at least, as long as the velocity of the upper plate does not become too large: $V<V_2^*$). Therefore, for this system the effective friction force $F_{fr}(V)$ will coincide with $f(V)$.

The presence of thermal noise changes the situation dramatically. When the velocity V is small enough, the stochastic force can excite the liquid sufficiently for the velocity distribution to cross the line $v(x)=V/2$, so the system does not evolve to any of the two attractors (14a) and (14b). The spatiotemporal fluctuating structure, determined by nonlinear properties of the system and induced by thermal noise, is developed, and $F_{fr}(V)$ differs significantly from $f(V)$. Scaling arguments would suggest that this occurs when $\Gamma \gtrsim cV^2$ or $\Gamma' \gtrsim (V/c)^2$. Thus such noise induced fluctuations will be most easily developed at low velocities V. When the upper plate moves with significantly higher velocities, the thermal excitation becomes relatively small, but, if the confined fluid is already excited and the velocity distribution crosses the line $v(x)=V/2$, the spatiotemporal fluctuations will persist. This means that to observe this fluctuating structure, when simulating the dynamics of the fluid for relatively large V and relatively small Γ, we need to choose the initial velocity distribution to be close to $v_0(x)=V/2$, and the dynamic evolution of the fluid will be completely different compared to the evolution from the initial condition $v_0(x)=0$ when the film will stick to the lower interface. This strong dependence of the evolution on initial conditions is the generic behavior in complex nonlinear dynamic systems. The fact that this type of behavior may be relevant to the physics of friction in thin lubricating films is, however, surprising.

We numerically integrated the hydrodynamic equations of motion for several different values of thermal noise and for a wide range of velocities of the moving plate V. The initial conditions $v_0(x)=V/2$ and $m_0(x)=0$ were taken in all these calculations, as argued above.

Figure 2 represents the effective temperature dependent friction forces $F_{fr}(V)$ for three different values of thermal noise: $\Gamma=0.002$, 0.005, and 0.01. As we showed in Sec. III, these values of Γ correspond to experimentally reasonable temperatures of order of magnitude of a room temperature. It can be seen that the functional dependence $F_{fr}(V)$ in the presence of temperature differs significantly from $f(V)$, especially at small velocities.

Figures 3–5 present the velocity and density distributions for $\Gamma=0.002$ and three different values of V: 0.002, 0.12, and 0.2. These three cases give three distinct types of behavior of the system when $V<V_1^*$, $V\approx V_1^*$, and $V>V_1^*$. In the first case, $V=0.002$ [Fig. 3(a)], the stationary solution (14c) is unstable and the system tends to build a spatiotemporal structure with the velocity oscillating between two attractors $v(x)=0$ and $v(x)=V$. However, the thermal noise in this case is relatively large and the dynamics is basically determined by the stochastic term. Nevertheless, the density fluctuations [Fig. 3(b)] reveal some periodic structure of small amplitude on the background of the noise. It is easy to understand that the corresponding force $F_{fr}(V)$ has to be rather small because the velocity [Fig. 3(a)] strongly oscillates almost symmetrically around zero. This causes the second multiplier term in the integral in Eq. (16) to oscillate and to make the integral small.

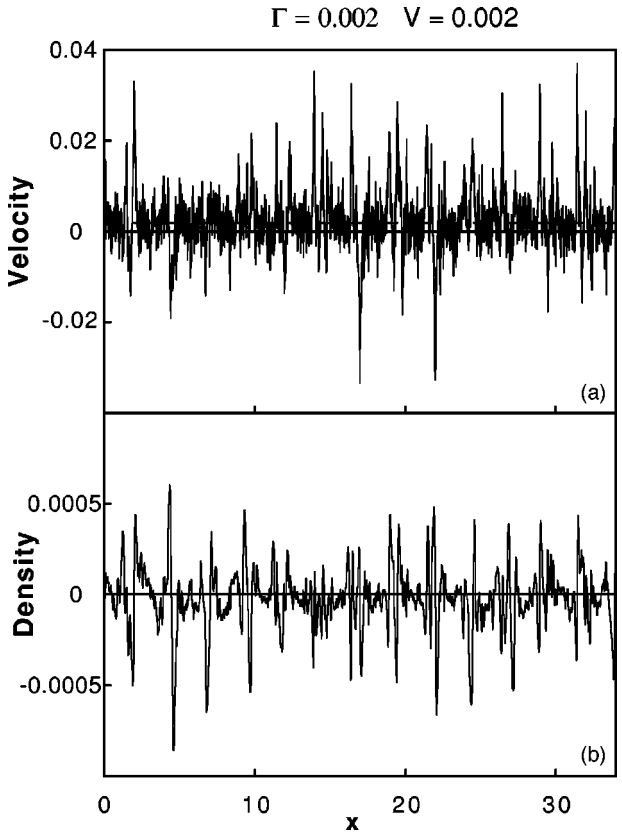

FIG. 3. (a) The velocity distribution and (b) the density distribution in the presence of temperature. $\Gamma=0.002$ and $V=0.002$.

In the case $V=0.12$ (Fig. 4), solution (14c) is neutrally stable. This is the case with the most pronounced structure in the velocity and, especially, in the density fluctuations. Since our natural spatial scale is c^2/F_0, the period of this structure is of order of magnitude of 10 μm. Indirect evidence of the existence of such large scale spatial structures in the thin film of a liquid lubricant was given in Ref. [10]; also see Refs. [3,4].

Finally, in the case $V=0.2$ (Fig. 5), solution (14c) is the attractor of the system. The thermal noise excites the fluid in the vicinity of this attractor, the amplitude of the resulting periodic structure in density fluctuations being more than one order of magnitude smaller than in the previous case.

Figure 6 shows the dependence of the amplitude $A=\sqrt{\langle m^2\rangle}$ of the density fluctuations on the velocity V for several values of the thermal noise Γ: 0.0001, 0.001, 0.002, and 0.005. The simulations clearly show that all the fluctuations have a peak for $V=V_1^*\approx 0.12$. For velocities $V>V_1^*$ the amplitude of the density fluctuations grows monotonically with Γ and decreases as V becomes larger.

This behavior can be understood by means of a linear expansion of hydrodynamic equations (8) and (9) around the state (14c) which, in this case, is the attractor. The linearized equations (8) and (9) are

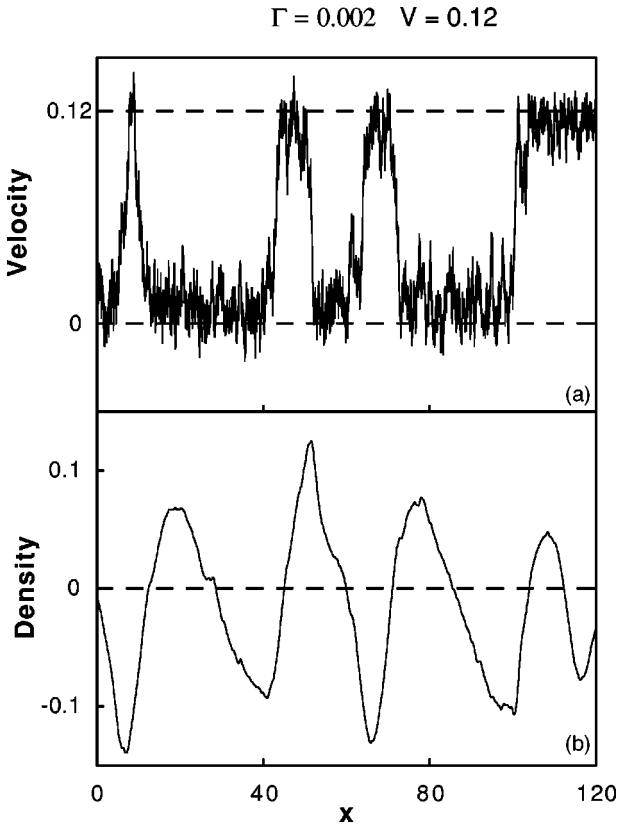

FIG. 4. (a) The velocity distribution and (b) the density distribution in the presence of temperature. $\Gamma=0.002$ and $V=0.12$.

$$u_t+\frac{V}{2}u_x+m_x=-\alpha(V)u+G(x,t), \tag{17a}$$

$$m_t+u_x+\frac{V}{2}m_x=0, \tag{17b}$$

where $u(x)=v(x)-V/2$, and

$$\alpha(V)=[f(v)+f(v-V)]'_{v=V/2}=2\left[K-b\Big/\left(\frac{bV}{2}+1\right)^2\right]. \tag{18}$$

Note that as $V\rightarrow V_1^*$ critical slowing down occurs: $\alpha(V)\approx\alpha_0(V-V_1^*)$, with $\alpha_0>0$.

Fourier transforming equations (17a) and (17b) and considering the dynamics of the individual modes, we obtain

$$|m_{k\omega}|^2=\frac{k^2|G_{k\omega}|^2}{|(\omega-kV/2)^2+i\alpha(V)(\omega-kV/2)-k^2|^2}. \tag{19}$$

Here $m_{k\omega}$ and $G_{k\omega}$ are Fourier transforms of $m(x,t)$ and $G(x,t)$, respectively. Thus

$$\langle m(x,t)^2\rangle=\int\frac{dk}{2\pi}\frac{d\omega}{2\pi}\langle|m_{k\omega}|^2\rangle. \tag{20}$$

Finally as Eq. (7) yields $\langle|G_{k\omega}|^2\rangle=2\Gamma$, we obtain

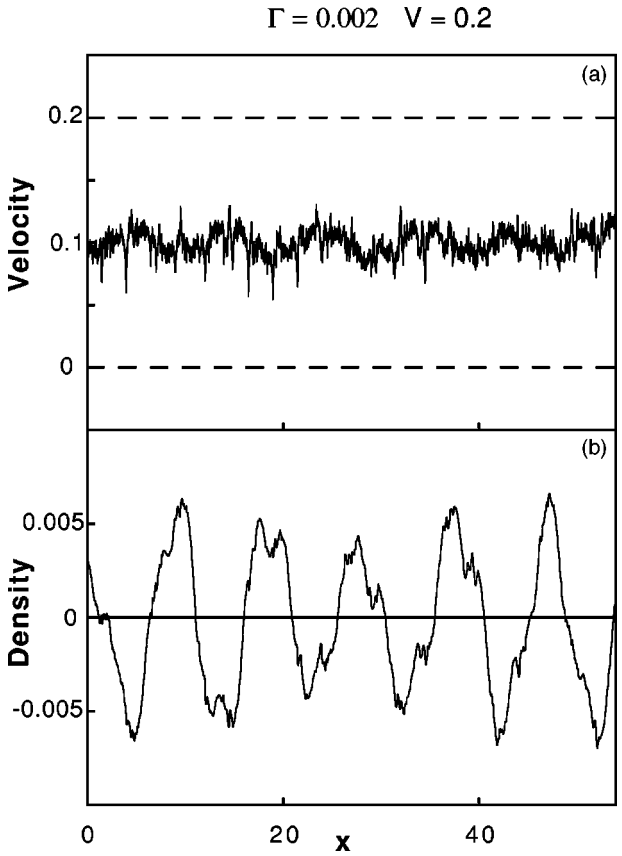

FIG. 5. (a) The velocity distribution and (b) the density distribution in the presence of temperature. $\Gamma=0.002$ and $V=0.2$.

$$\langle m(x,t)^2\rangle=\frac{\Gamma}{\pi^2}\int_0^\Lambda k^2dk\times\int_{-\infty}^{\infty}\frac{d\omega}{|(\omega-kV/2)^2+i\alpha(V)(\omega-kV/2)-k^2|^2}. \tag{21}$$

The ultraviolet limit to the k integration in Eq. (21) will be set by some microscopic length scale $a(\Lambda\sim2\pi/a)$ at which

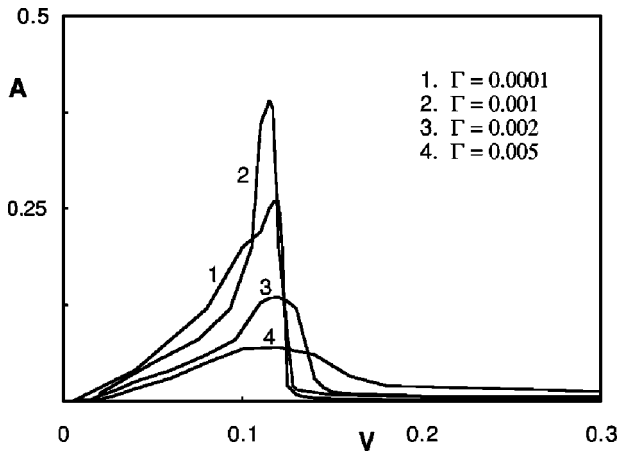

FIG. 6. The dependence of the amplitude $A=\sqrt{\langle m^2\rangle}$ of the density fluctuations on a driving velocity V and a strength of thermal noise Γ.

the resultant large spatial gradients which will occur at this inner scale break the validity of the linear approximation. Integrating Eq. (21), we are then able to estimate the basic qualitative dependence of the amplitude of the density fluctuations on Γ and V. We obtain

$$\langle m^2 \rangle = \frac{\Gamma}{\pi \alpha(V)} \int_0^{\Lambda} dk = \frac{\Gamma \Lambda}{\pi \alpha(V)}. \tag{22}$$

Note that according to Eqs. (22) and (18) the density fluctuations grow with Γ, diverging as $1/\sqrt{V - V_1^*}$ as $V \to V_1^*$, and tend to a constant when V becomes large enough. All these facts are consistent with our numerical results.

For velocities $V < V_1^*$ the dependence of the density fluctuations on Γ is just the opposite: the amplitude decreases monotonically with increasing Γ. This can be understood if we recall that in this case the solutions $v(x) = V/2$ and $m(x) = 0$ are unstable. This means that in the absense of thermal noise we already have a spatiotemporal structure appearing due to the nonlinear interactions present, and concurrent switching between the basins of attraction of solutions (14a) and (14b). Thermal noise only destroys this structure, in contrast with the previous case, where it helped to build one.

Finally for $V = V_1^*$ the dependence of the amplitude of the density fluctuations on Γ is not monotonic, as can be seen from Fig. 6. The simulations show that the most pronounced fluctuations occur for a specific value of Γ_{max}. In Fig. 6, $\Gamma_{max} \approx 10^{-3}$. This value of the ''optimal'' noise strength is determined by a subtle relationship between V and Γ, which is similar to the well-known phenomenon of stochastic resonance where the cooperation between the external drive and the thermal noise leads to the appearance of well-pronounced maxima in the temporal response of a dynamical system.

V. CONCLUSIONS

Coherent structures appear at the mesoscale in molecularly thin films of liquid lubricant when driven between two relatively sliding plates in the presence of stick-slip boundary conditions. The spatiotemporal structures which may develop in thin lubricating films under shear is a topic of a great interest now [3,10,11]. We observed in our simulations that the induced density fluctuations are a strong function of the thermal noise, and can change by several orders of magnitude. This is similar to the well-known phenomenon of stochastic resonance where the cooperation between the external drive and the thermal noise leads to the appearance of resonant drift in Langevin equations, but here the cooperation between noise and drive creates well-pronounced spatiotemporal structures.

Such coherent stuctures are also likely to appear in two-dimensional hydrodynamic studies based on Eqs. (1) and (3). They will have a strong influence on the resulting lubricating properties of thin films as the temperature is varied. Specifically, at low velocities we observed a reduction in friction with increasing thermal noise. Such a dependence of friction on temperature is well known in the literature [28,3], but it has mainly been ascribed to phase transitions in the film of a lubricant, while our analysis suggests that anomalous dissipation is a consequence of the development of noise-induced coherent structures.

[1] J. Krim, MRS Bull. **23**, 6 (1998).

[2] D. Tabor, in *Microscopic Aspects of Adhesion and Lubrication, Tribology Series*, edited by J. M. Georges (Elsevier, New York, 1982), Vol. 7, p. 651.

[3] B. Bhushan, J. N. Israelachvili, and U. Landman, Nature (London) **374**, 607 (1995).

[4] S. Granick, Phys. Today **52**(7), 26 (1999).

[5] J. Krim, D. H. Solina, and R. Chiarello, Phys. Rev. Lett. **66**, 181 (1991).

[6] J. N. Israelachvili and D. Tabor, Nature (London) **241**, 148 (1973).

[7] J. Klein and E. Kumacheva, Science **269**, 816 (1995).

[8] J. V. Alsten and S. Granick, Phys. Rev. Lett. **61**, 2570 (1988).

[9] S. Granick, Science **253**, 1374 (1991).

[10] A. L. Demirel and S. Granick, Phys. Rev. Lett. **77**, 4330 (1996).

[11] A. Dhinojwala, L. Cai, and S. Granick, in *Dynamics in Small Confining Systems III*, edited by J. M. Drake, J. Klafter, R. Kopelman, MRS Symposia Proceedings No. 469 (Materials Research Society, Pittsburgh, 1997), p. 49.

[12] Y. Braiman, F. Family, and H. G. E. Hentschel, Phys. Rev. E **53**, R3005 (1996).

[13] Y. Braiman, F. Family, and H. G. E. Hentschel, Phys. Rev. B **55**, 5491 (1997).

[14] M. G. Rozman, M. Urbakh, and J. Klafter, Phys. Rev. Lett. **77**, 683 (1996).

[15] B. N. J. Persson, Phys. Rev. B **48**, 18 140 (1993).

[16] B. N. J. Persson, J. Chem. Phys. **103**, 3849 (1995).

[17] A. M. Homola, J. N. Israelachvili, M. L. Gee, and P. M. McGuiggan, ASME J. Tribol. **111**, 675 (1989).

[18] R. Burridge and L. Knopoff, Bull. Seismol. Soc. Am. **57**, 341 (1967).

[19] J. M. Carlson and J. S. Langer, Phys. Rev. A **40**, 6470 (1989).

[20] M. Cieplak, E. D. Smith, and M. O. Robbins, Science **265**, 1209 (1994).

[21] E. D. Smith, M. O. Robbins, and M. Cieplak, Phys. Rev. B **54**, 8252 (1996).

[22] M. Peyrard and S. Aubry, J. Phys. C **16**, 1593 (1983).

[23] T. Baumberger, F. Heslot, and B. Perrin, Nature (London) **367**, 544 (1994).

[24] T. Baumberger, C. Caroli, B. Perrin, and O. Ronsin, Phys. Rev. E **51**, 4005 (1994).

[25] F. Heslot, T. Baumberger, B. Perrin, B. Caroli, and C. Caroli, Phys. Rev. E **49**, 4973 (1994).

[26] D. Pisarenko and P. Mora, Pure Appl. Geophys. **142**, 447 (1994).

[27] L. Landau and E. Lifshitz, *Fluid Mechanics* (Pergamon Press, London, 1989).

[28] H. Yoshizawa, Y. L. Chen, and J. Israelachvili, J. Phys. Chem. **97**, 4128 (1993).